POLISH JOURNAL *of* RADIOLOGY

Original paper

Diagnostic models for the detection of intrauterine growth restriction and placental insufficiency severity based on magnetic resonance imaging of the placenta

Behnaz Moradi[1,2,A,B,D,E,F], Elnaz Tabibian[3,C,D,E,F], Mohammad Ali Kazemi[4,2,A,D,E], Mahboobeh Shirazi[5,A,B,D], Mohammadreza Chavoshi[6,C,D,E], Sina Rashedi[7,C,D,E]

[1]Department of Radiology, Women's Yas Hospital, Tehran University of Medical Sciences, Tehran, Iran
[2]Advanced Diagnostic and Interventional Radiology Research Center (ADIR), Tehran University of Medical Sciences, Tehran, Iran
[3]Department of Radiology, Tehran University of Medical Sciences, Tehran, Iran
[4]Department of Radiology, Amiralam Hospital, Tehran University of Medical Sciences, Tehran, Iran
[5]Maternal, Foetal and Neonatal Research Centre, Women's Yas Hospital, Tehran University of Medical Sciences, Tehran, Iran
[6]Department of Radiology, Shariati Hospital, Tehran University of Medical Sciences, Tehran, Iran
[7]School of Medicine, Tehran University of Medical Sciences, Tehran, Iran

Abstract

Purpose: We aimed to provide diagnostic models based on different parameters of placental magnetic resonance imaging (MRI) to detect intrauterine growth restriction (IUGR), as well as the severity of placental insufficiency.

Material and methods: We included 44 foetuses with appropriate weight for gestational age (AGA) and 46 foetuses with documented IUGR, defined as the estimated foetal weight (EFW) below the 10th centile. Using Doppler ultrasound, IUGR cases were divided into 2 groups: 1) IUGR with severity signs: EFW < 3rd centile, or cerebroplacental ratio < 5th centile, or abnormal umbilical/uterine artery pulsatility index; and 2) non-severe IUGR without any of this criterion. For all these participants, placental MRI was performed in the third gestational trimester, and its parameters were compared between AGA and IUGR, as well as between the severe and non-severe IUGR groups. Two diagnostic models consisting of significant predictors were developed, and their performance was investigated with accuracy metrics.

Results: The severity signs were detected in 25 (54.3%) IUGR cases. The diagnostic model for the differentiation of IUGR from AGA revealed an acceptable performance (area under the curve [AUC] of 0.749) and consisted of 2 variables: 1) the largest size of infarct ≥ 25 mm (odds ratio [OR] = 5.01, $p = 0.001$), and 2) thickness : volume ratio ≥ 0.043 (OR = 3.76, $p = 0.027$); while, the logistic regression model for detection of the severity signs was even better, with AUC = 0.862, and comprised of 2 predictors: 1) placental infarct percent ≥ 10% (OR = 26.73, $p = 0.004$), and 2) placental globular shape (OR = 5.40, $p = 0.034$).

Conclusions: Placental MRI parameters can differentiate IUGR from AGA, and more precisely, assess the severity of placental insufficiency in IUGR foetuses.

Key words: ultrasonography, magnetic resonance imaging, foetal growth retardation, diagnostic tool assessment.

Correspondence address:
Elnaz Tabibian, Assistant Professor in Department of Radiology, Medical Imaging Centre, Imam Khomeini Hospital Complex, End of Keshavarz Blvd., Tehran, Iran, postal code: 1419733141, phone: +98-21-61190, e-mail: elnaz.tabibian@gmail.com

Introduction

Intrauterine growth restriction (IUGR), characterized by failure of the foetus to reach its potential growth, is associated with increased risk of preterm delivery, adverse perinatal outcomes, stillbirth, and neurodevelopmental delay in the long term [1,2]. Although complex aetiological parameters have been suggested, placental insufficiency is regarded as the primary cause of IUGR [2]. This phenomenon is related to the shallow invasion of the trophoblast into maternal tissue and insufficient conversion of the spiral arterioles, resulting in placental ischaemia [3]. The ultrasound-based methods of foetal growth quantification alongside Doppler measurement in the umbilical arteries are considered as the mainstays of IUGR detection. These modalities can also aid in the timing of delivery of foetuses with IUGR [4].

However, the diagnostic accuracy of these ultrasound-based techniques for IUGR identification in late gestation is relatively poor, with sensitivities as low as 15% to 50% [5,6]. This insensitive detection of placental dysfunction is assumed to be a result of the inadequate correlation between umbilical artery Doppler measures and foetal growth restriction [7]. Indeed, severe impairment of placental blood flow is required for significant alterations in umbilical Doppler values to become evident. Therefore, complementary investigations are warranted for further assessment of pregnancies complicated by IUGR.

As an adjunct to ultrasound, foetal magnetic resonance imaging (MRI) is currently considered an established diagnostic modality for the detection of intrauterine abnormalities. Since the first clinical utilization of MRI for evaluation of placenta in patients suspected of placenta previa in 1986 [8], its role has expanded to various obstetric aspects ranging from the investigation of placental invasion in cases of placenta accreta/increta/percreta [9] to the delineation of morphological deformities and placental perfusion using diffusion-weighted imaging (DWI) sequences [10]. It has been demonstrated that MRI assessments can detect a wide spectrum of placental pathologies from haemorrhages to infarctions and, more importantly, placental insufficiency [11]. Furthermore, several MRI findings such as placental volume and extent of pathological involvement have been verified to associate with the severity of placental insufficiency [12-14]. Despite these promising results, few attempts have been made to propose MRI-based models for the detection and severity assessment of patients with IUGR. Hence, we aimed to provide diagnostic models based on different parameters of placental MRI to detect IUGR, as well as the severity of placental insufficiency.

Material and methods

Patient population and Doppler ultrasound examination

Our institutional review board approved the study, and written informed consent was obtained from all pregnant women who participated in the study. Ethical approval was obtained from the Women's *Yas* Hospital Research Ethics Committee (Rec No: 98-01-98-41442), and the study was conducted in accordance with the declaration of Helsinki [15]. Between 2017 and 2019, all pregnant women with pregnancies complicated by IUGR, defined as the estimated foetal weight (EFW) below the 10th percentile based on ultrasonographic findings, were assessed [16]. Gestational age for all foetuses was estimated based on the first-trimester crown-rump length. Exclusion criteria were defined as (1) multiple pregnancies [6 cases], (2) the presence of placenta accreta spectrum [2 cases], (3) the presence of intrauterine infections [1 case], (4) contraindications for MRI [1 case], and (5) refusal to sign informed consent for foetal MRI [2 cases]. Also, we lost 2 foetuses with severe vascular impairment because of emergent caesarean delivery. Ultimately, 46 singleton pregnancies with documented IUGR were recruited for placental MRI evaluation in the third gestational trimester (IUGR cohort).

The transabdominal Doppler ultrasound was carried out employing a 2-6 MHz curved-array transducer (Affinity 50, General imaging configuration, Philips ultrasound machine, USA) for all patients of this cohort in the third trimester. The EFW, as well as umbilical artery (UA), mean bilateral uterine artery (UtA), and middle cerebral artery (MCA) pulsatility indices, were measured and assessed according to the reference chart [17]. Additionally, the cerebroplacental ratio was calculated by dividing the pulsatility index of MCA by the UA pulsatility index. By means of this ultrasound-based evaluation, the IUGR cohort was divided into 2 groups: 1) IUGR with severity signs: EFW < 3rd centile, and/or cerebroplacental ratio < 5th centile, and/or UA or UtA pulsatility index > 95th centile; and 2) non-severe IUGR without any of these criteria [18].

Another cohort of participants with the same exclusion criteria consisted of 44 foetuses with appropriate weight for gestational age (AGA) defined as EFW ≥ 10th centile based on sonographic measurements, matched with the IUGR cohort regarding the maternal and gestational age, were also included to serve as the control group (AGA cohort). These foetuses were selected from pregnant women who were referred for MRI due to suspected abnormalities based on the prenatal ultrasound on the central nervous system (the majority of cases), pulmonary system, genitourinary, and gastrointestinal tracts. The gestational age was based on a reliable recollection of the last menstrual period, alongside ultrasonographic confirmation within the first gestational trimester. All the included patients were followed until the end of the neonatal period, and the data concerning maternal and foetal features were gathered.

Magnetic resonance imaging acquisition and interpretation

All foetuses were examined with a 3T MR unit General Electric system (GE Healthcare, discovery 750 GEM), using

a 16-channel-phased array coil following 4 hours of maternal fasting. As demonstrated previously, exposure to 3T magnetic fields applied in the clinical MRI process does not pose any adverse effects to the foetus [19,20]. The placental MRI was performed while the participants were in the left lateral decubitus position within the same week of ultrasound. The duration of performing placental MRI was 30 ± 5 minutes. The examination protocol consisted of conventional sequences for all women including 4 mm single-shot fast spin-echo T2-weighted sequences in 3 orthogonal planes and axial fast multiplanar spoiled gradient-recalled acquisition in the steady-state T1-weighted sequences in an axial plane. Only T1-weighted sequences were performed with breath-holding. DWI sequences were performed through the placental surface (b-value, 0-800 s/mm² in 3 orthogonal axes [x, y, z]) in the coronal plane without breath-holding. The apparent diffusion coefficient (ADC) measurements on matched coronal DWI were performed. Offline analyses of all morphologic and biometric placental measurements were performed on an Infinite Picture Archiving and Communication System (PACS) and by drawing a freehand region of interest (ROI).

The MRI images of the placenta were assessed for the presence of placental infarct (an area of low T2 signal or high T2 signal with low T2 rim), its number, the largest size, and involvement percentage in T2-weighted images. The involvement percent of the placenta by infarcts was assessed subjectively as 0%, 5%, and up to 100%. Retroplacental bleeding was assessed in a T1-weighted sequence. The placenta shape was also recorded as globular or plate-like based on the rounded appearance of its margin (Figure 1).

Placental signal intensity in T1- and T2-weighted sequences and ADC in DWI images relative to the amniotic fluid signal intensity in these sequences were assessed. The signal intensity and ADC of the placenta were measured by drawing the 2 largest possible ROIs in the centre (near cord insertion) and 2 ROIs at the periphery of the placenta (up to 2 cm to the placental edge), and the average of them was recorded for the central and peripheral site (Figure 2). The central and peripheral signal intensities were divided by the amniotic fluid signal intensity in T1- and T2-weighted sequences to obtain central and peripheral ratios.

Maximal placental thickness was taken as the thickest point of the placenta, usually near the central umbilical cord insertion. Placental volume was assessed by manually drawing the ROIs on each slice. Then the sum of the placental area of each slice was multiplied by the sum of the slice thickness and slice gap to calculate the volume. The largest placental area was also recorded (Figure 2).

All morphologic and biometric analyses were conducted by a 6-year experienced radiologist (the first author) blinded to the patients' characteristics. In the case of motion artifact, the sequence was repeated until the acceptable image was acquired.
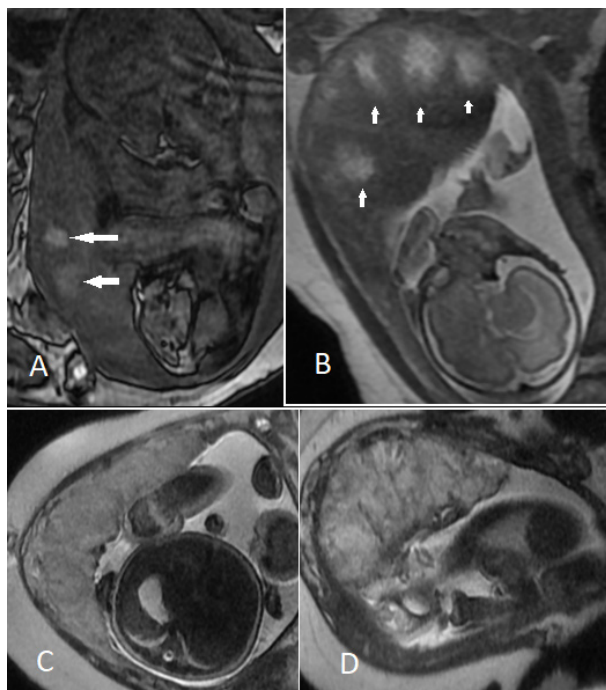

Figure 1. A) Retroplacental haemorrhage (arrows) in T1-weighted image in a 34-week foetus with clinically non-significant intrauterine growth restriction (IUGR). **B**) Multiple placental infarcts (arrows) with a central high and low peripheral rim of T2 signal intensity in a 35-week foetus with increased umbilical artery pulsatility index. **C**) Placenta with plate-like shape in a 37-week foetus with clinically non-significant IUGR. **D**) Placenta with globular shape in a 34-week foetus with clinically significant IUGR
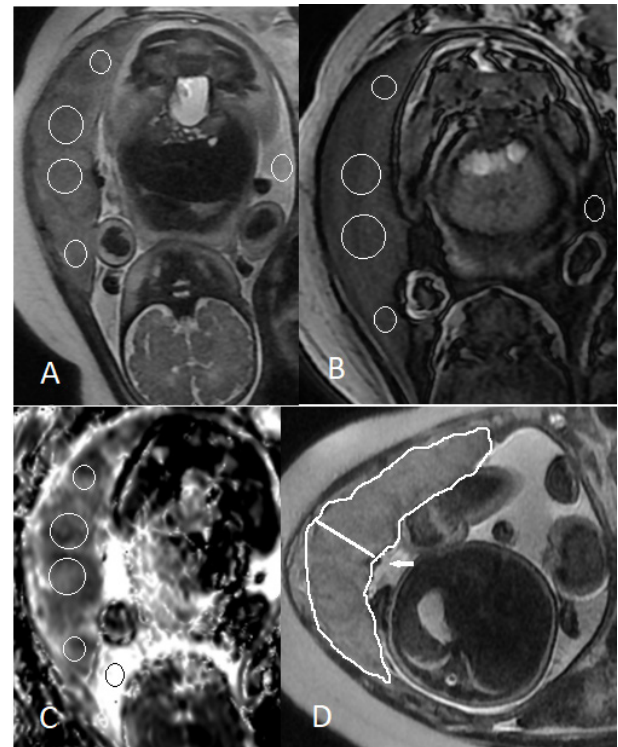

Figure 2. Assessment of placental and amniotic fluid signal intensities in (**A**) T2-weighted, (**B**) T1-weighted, and (**C**) apparent diffusion coefficient (ADC) map by the placement of 2 central and 2 peripheral regions of interest (ROIs). **D**) Measurement of placental thickness and the largest area near the cord insertion site (arrow)

Statistical analysis

The categorical variables were summarized as numbers and percentages and were compared using the χ^2 test. The continuous variables were presented as mean ± standard deviation (SD) and were analysed between 2 cohorts using an independent samples *t*-test and among 3 cohorts using the analysis of variance (ANOVA) method. In the case of a significant difference using the ANOVA method, post hoc analysis with the Bonferroni statistic was implemented to detect the source of difference.

For model development regarding the diagnosis of IUGR, the MRI parameters were compared between AGA and IUGR cohorts. These parameters were then compared between the 2 IUGR cohorts (severe and non-severe based on Doppler ultrasound) to assess the severity of placental insufficiency. According to these results, we determined the main predictors for both IUGR detection and severity assessment (those that had *p*-values less than 0.10). Categorical and continuous variables were investigated in univariate analysis, and their odds ratios (ORs) and corresponding 95% confidence intervals (CIs) were calculated. Also, based on the cut-off values for each MRI parameter (with the best accuracy in receiver operating characteristic [ROC] curve), quantitative MRI parameters were converted into categorical ones. The variables with significant discriminating values in univariate analysis were then included in multivariate analysis (those with *p*-value < 0.05). Only one of the variables (categorical or continuous) for each MRI parameter that demonstrated a better predictor value was considered in multivariate analysis. The final prediction models consisted of all the MRI parameters that remained significant in multivariate analysis ($p < 0.05$). Eventually, the accuracy for both models was investigated by ROC curves and calculation of area under the curves (AUCs). All the analyses were performed using Stata (version 13.1; Stata Corp., Texas, USA).

Results

A total of 90 foetuses (46 IUGR and 44 AGA), with foetal age ranging from 26 to 39 weeks at the time of MRI investigation, were included. Among the patients in the IUGR cohort, 25 (54.34%) were categorized as severe cases according to the criteria previously mentioned. Two severely growth-restricted foetuses died during the third gestational trimester (both at 32 weeks of gestation). Table 1 presents the maternal, foetal, and neonatal characteristics of the AGA cohort and 2 cohorts of IUGR patients. No significant difference was noted except for the foetal gender ($p = 0.047$, more female foetuses in the non-severe IUGR cohort) and maternal drug history ($p = 0.002$, less positive drug history in the AGA cohort). Expectedly, there was also a significant difference between the groups in terms of EFW ($p = 0.026$, significantly higher in AGA) and birth weight ($p < 0.001$) between these 3 cohorts. Regarding MRI fea-

tures, 9 parameters were significantly different between the 3 cohorts (Table 2): 1. Central ADC ($p = 0.049$, lower in severe IUGR), 2. Peripheral ADC ($p = 0.006$, lower in severe IUGR), 3. Infarct number ($p < 0.001$, higher severe IUGR), 4. The largest size of infarct ($p < 0.001$, higher in severe IUGR), 5. Involvement percentage with infarct ($p < 0.001$, higher in severe IUGR), 6. Placental thickness ($p = 0.04$, higher in severe IUGR), 7. Thickness-to-volume ratio ($p = 0.01$, higher in severe IUGR), 8. Placental shape ($p = 0.001$, more globular in severe IUGR), and 9. Bleeding ($p = 0.011$, higher chance in severe IUGR) (Figure 3).

For IUGR detection, 6 variables were identified in univariate analysis to be further explored in multivariate analysis (Table 3): 1. Infarct number (OR = 1.38, $p = 0.002$), 2. Placental globular shape (OR = 2.44, $p = 0.047$), 3. Bleeding (OR = 8.84, $p = 0.044$), 4. The largest size of infarct ≥ 25 mm (OR = 5.63, $p < 0.001$), 5. Involvement percent with infarct ≥ 10% (OR = 4.90, $p < 0.001$), and 6. Thickness-to-volume ratio ≥ 0.043 (OR = 4.57, $p = 0.007$). Among these, only 2 variables remained significant in multivariate analysis: 1. The largest size of infarct ≥ 25 mm (OR = 5.01, 95% confidence interval [CI] [1.95-12.85]; $p = 0.001$), and 2. Thickness-to-volume ratio ≥ 0.043 (OR = 3.76, 95% CI [1.16-12.23]; $p = 0.027$) (Table 4). The ROC curve analysis for this diagnostic model exhibited acceptable accuracy (AUC = 0.749; accuracy = 70.0%; sensitivity = 65.2%; specificity = 75.0%; negative predictive value (NPV) = 67.3%; positive predictive value (PPV) = 73.1%) (Figure 4).

Concerning the severity of placental insufficiency in IUGR patients, 7 MRI parameters correlated with severity in univariate analysis (Table 3): 1. Peripheral T2 ratio (OR = 124.1, $p = 0.017$), 2. Peripheral ADC (OR = 1.00, $p = 0.017$), 3. Infarct number (OR = 1.83, $p = 0.002$), 4. The largest size of infarct (OR = 1.07, $p = 0.009$), 5. Placental globular shape (OR = 6.80, $p = 0.004$), 6. Involvement percent with infarct ≥ 10% (OR = 32.0, $p = 0.002$), and 7. Thickness-to-volume ratio ≥ 0.035 (OR = 4.40, $p = 0.026$). In the final model, 2 variables were considered as independent predictors of IUGR severity: 1. Placental globular shape (OR = 5.40, 95% CI [1.13-25.75]; $p = 0.034$), and 2. Involvement percent with infarct ≥ 10% (OR = 26.73, 95% CI [2.77-257.76]; $p = 0.004$) (Table 4). This model reached better accuracy with the AUC = 0.862 (accuracy = 78.2%; sensitivity = 68.0%; specificity = 90.4%; NPV = 70.3%; PPV = 89.4%) (Figure 4).

Discussion

Our study has demonstrated that MRI of the placenta with a diagnostic model consisting of 2 predictors (the largest infarct size and thickness-to-volume ratio) can detect IUGR with relatively good accuracy. For severity assessment of placental insufficiency in foetuses suffering from IUGR, placental globular shape, and involvement percentage with infarct based on placental MRI achieved a superior accuracy (with an AUC of more than 0.8). To our knowledge,

Table 1. Characteristics of the study population across the groups

Factor		I: AGA (n = 44)	II: Non-severe IUGR (n = 21)	III: Severe IUGR (n = 25)	Total (n = 90)	p-value
Maternal characteristics						
Age		31.12 ± 4.46	29.48 ± 4.20	29.88 ± 5.68	30.38 ± 4.78	0.364
Height (cm)		162.03 ± 10.35	162.00 ± 4.43	161.64 ± 5.60	161.90 ± 7.78	0.980
Weight (kg)		77.08 ± 12.61	75.81 ± 11.29	78.96 ± 14.92	77.33 ± 12.94	0.710
BMI (kg/m²)		29.63 ± 6.01	28.93 ± 4.41	30.21 ± 5.59	29.63 ± 5.47	0.736
Smoking	Yes	0 (0.0)	0 (0.0)	0 (0.0)	0 (0.0)	NA
	No	44 (100)	21 (100)	25 (100)	90 (100)	
Past medical history	No disease	40 (90.9)	17 (81.0)	21 (84.0)	78 (86.6)	0.489
	Chronic conditions (hypothyroidism, etc.)	4 (9.1)	4 (19.0)	4 (16.0)	12 (13.7)	
Drug history	No drug	40 (90.9)	13 (61.9)	14 (56.0)	67 (74.4)	0.002
	Any medication (mostly levothyroxine)	4 (9.1)	8 (38.1)	11 (44.0)	23 (25.6)	
Foetal characteristics						
Foetal age (weeks)		32.45 ± 2.48	33.43 ± 3.66	33.72 ± 2.33	33.03 ± 2.79	0.149
Estimated foetal weight (g)		1999.07 ± 463.52	1775.48 ± 560.99	1637.24 ± 406.02	1810.84 ± 494.04	0.026
Gender	Female	15 (34.1)	14 (67.6)	11 (44.0)	40 (44.4)	0.047
	Male	29 (56.9)	7 (33.4)	14 (56.0)	50 (55.6)	
Death	Yes	0 (0)	0 (0)	2 (8.0)	2 (2.2)	0.070
	No	44 (100)	21 (100)	23 (92.0)	88 (97.8)	
Neonatal characteristics						
Birth weight (g)		3058.53 ± 694.26	2670.47 ± 263.60	2178.18 ± 614.93	2701.17 ± 684.56	< 0.001
Gestational age (weeks)		37.80 ± 2.35	37.68 ± 0.88	36.76 ± 1.89	37.46 ± 1.94	0.145
Apgar score	< 7	0 (0)	0 (0)	2 (8.0)	2 (2.2)	0.070
	≥ 7	44 (100)	21 (100)	23 (92.0)	88 (97.8)	
Neonatal acidosis	Yes	12 (27.3)	8 (38.1)	12 (48.0)	32 (35.5)	0.216
	No	32 (72.7)	13 (61.9)	13 (52.0)	58 (64.5)	
NICU admission	Yes	8 (18.2)	4 (19.0)	10 (40.0)	22 (24.4)	0.103
	No	36 (81.8)	17 (81.0)	15 (60.0)	68 (75.5)	

BMI – body mass index, IUGR – intrauterine growth restriction, NA – not applicable, NICU – neonatal intensive care unit
Continuous variables are presented as mean ± standard deviation, categorical variables as number (%).

this is one of the first studies to propose prediction models based on placental MRI features for diagnosis, as well as severity assessment of IUGR.

Recent studies have demonstrated placental perfusion reduction in IUGR patients using DWI and contrast-enhanced placental perfusion mapping [12,14,21-23]. Gorkem *et al.* recently investigated the placental diffusion difference in IUGR patients with worsening Doppler ultrasound features and concluded that placental ADC values have the ability to predict IUGR severity with comparable accuracy to the UA pulsatility index [14]. Moreover, placental diffusion alteration has been detected at the early phases of IUGR onset in contrast to the UA pulsatility index [14]. These results suggest a possible role of MRI-based methods in the management of patients with IUGR. In our study, although placental ADC values were significantly correlated with IUGR severity in univariate analysis, it was denoted that placental morphological parameters (placental shape and involvement percentage with infarct) were better predictors after further investigation by multivariate analysis. This could be because more profound and long-standing alterations in placental perfusion are required for placental morphological abnormalities to occur. Therefore, morphological abnormalities denote more severe perfusion reduction, which is linked to more severe growth restriction. Although volumetric evaluation of the placenta can be conducted during the first trimester using 3D ultrasound, due to limitations in the field of view, it becomes increasingly difficult in the course of time [13].

Table 2. Comparison of MRI parameters across the subgroups

Factor		I: AGA (n = 44)	II: Non-severe IUGR (n = 21)	III: Severe IUGR (n = 25)	IV: Total IUGR (n = 46)	V: Total (n = 90)	p-value[a]	p-value[b]	p-value[c]
Central T2 ratio		0.659 ± 0.20	0.676 ± 0.19	0.566 ± 0.17	0.616 ± 0.18	0.637 ± 0.19	0.105	0.315	**0.048**
Peripheral T2 ratio		0.587 ± 0.19	0.634 ± 0.16	0.508 ± 0.15	0.566 ± 0.16	0.576 ± 0.18	0.052	0.585	0.011
Central T1 ratio		1.694 ± 0.36	1.840 ± 0.74	1.783 ± 0.48	1.810 ± 0.61	1.754 ± 0.51	0.536	0.291	0.761
Peripheral T1 ratio		1.745 ± 0.46	1.786 ± 0.77	1.701 ± 0.39	1.741 ± 0.59	1.743 ± 0.53	0.869	0.972	0.639
Central ADC (mm²/s)		1858.33 ± 375.22	2051.88 ± 360.89	1693.04 ± 538.36	1840.26 ± 501.18	1847.14 ± 454.15	**0.049**	0.880	**0.025**
Peripheral ADC (mm²/s)		1675.08 ± 336.54	1935.56 ± 291.02	1515.22 ± 476.86	1687.67 ± 457.11	1682.87 ± 412.46	**0.006**	0.908	**0.003**
Amniotic fluid ADC (mm²/s)		3733.33 ± 976.98	3830.62 ±1220.03	4039.57 ± 1096.77	3953.85 ± 1137.90	3869.84 ± 1076.72	0.621	0.434	0.579
Infarct number		2.11 ±1.74	2.14 ± 1.98	5.44 ± 2.97	3.93 ± 3.03	3.04 ± 2.63	**< 0.001**	**0.001**	**< 0.001**
Largest size of infarct (mm)		17.14 ± 12.83	22.81 ± 16.91	37.24 ± 13.29	30.65 ± 16.56	24.04 ± 16.26	**< 0.001**	**< 0.001**	**< 0.001**
Involvement percentage with infarct		6.70 ± 7.92	7.86 ±8.74	24.60 ± 18.81	16.96 ± 17.14	11.94 ± 14.33	**< 0.001**	**0.001**	**< 0.001**
Placental volume (mm³)		1182.36 ± 197.12	1182.52 ± 280.29	1136.32 ± 317.66	1157.41 ± 298.79	1169.61 ± 253.12	0.746	0.640	0.607
Placental thickness (mm)		40.77 ± 8.93	42.00 ± 11.69	47.60 ± 12.59	45.04 ± 12.38	42.96 ± 10.98	**0.040**	**0.065**	0.127
Placental area (mm²)		6741.6 ± 1657.5	6154.3 ± 2271.5	6429.6 ± 1464.6	6303.9 ± 1859.2	6517.9 ± 1767.4	0.442	0.242	0.622
Thickness-to-volume ratio		0.035 ± 0.007	0.036 ± 0.008	0.046 ± 0.025	0.041 ± 0.015	0.038 ± 0.015	**0.010**	**0.038**	**0.094**
Placental shape	Plate-like	32 (72.7)	16 (76.1)	8 (32.0)	24 (52.2)	56 (62.3)	**0.001**	**0.044**	**0.003**
	Globular	12 (27.3)	5 (23.9)	17 (68.0)	22 (47.8)	34 (37.7)			
Bleeding	Yes	1 (2.3)	2 (9.5)	6 (24.0)	8 (17.4)	10 (12.5)	**0.011**	**0.031**	0.197
	No	42 (97.7)	19 (91.5)	19 (76.0)	38 (82.6)	70 (87.5)			

ADC – apparent diffusion coefficient, IUGR – intrauterine growth restriction.

Continuous variables are presented as mean ± standard deviation, categorical variables as number (%).

P-values less than 0.05 have been indicated in bold.

[a]Comparison among 3 columns of I, II, and III using ANOVA method. [b]Comparison between 2 columns of I and IV using the independent samples t-test. [c]Comparison between 2 columns of II and III using the independent samples t-test.
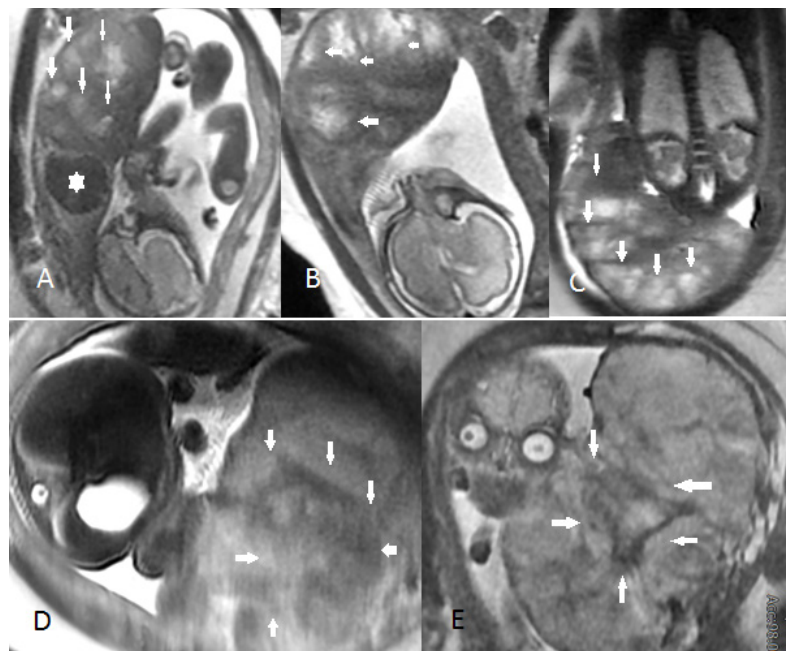

Figure 3. Five foetuses with clinically significant IUGR with impaired Doppler indices. **A-C)** Placenta with obvious globular shape, increased thickness, and multiple infarcts (arrows) in about 60-70% of total area. **D, E)** Two cases with thick placenta, approximately 68 and 70 mm, respectively, with an obvious globular shape and multiple large infarcts (arrows). The leiomyoma has been indicated by an asterisk

In this regard, placental MRI, with the larger field of view, multiplanar capabilities, and high-contrast images, can provide additional information about placental morphology and aid in managing growth-restricted foetuses.

Our findings regarding dysfunctional placenta with morphological and perfusion abnormalities are supported by histopathological studies that previously demonstrated that the frequency of apoptosis in intramural and endovascular trophoblast is increased in growth-restricted foetuses, and this focal loss of endovascular cells may lead to a rather globular placental shape and smaller dysfunctional placenta with larger infarct sizes [24,25]. During the first gestational trimester, poor trophoblastic invasion observed in IUGR patients re-

sults in chronic placental hypoxaemia, which also induces trophoblastic apoptosis [26,27]. These pathophysiological processes contribute to poor placental perfusion, thickened placenta with the globular structure instead of flattened disc-shaped appearance, and reduced placental volume with more involvement of reduced areas of infarct. In the third trimester after 24-28 weeks, the placenta continues to mature, becoming more heterogeneous with a growth in thickness. Multiple thin and hypointense lines increasingly appear and cross the perpendicular axis of the placenta, representing the interlobular septa, which separates normal cotyledons. These lobulated structures are surrounded by maternal blood, which can exchange oxygen and nutrients with the foetal blood in

Table 4. Final prediction models for detection and severity assessment of intrauterine growth restriction (IUGR) based on placental MRI features

	OR	95% CI	Standard error	Z scores	p-value
A. IUGR detection					
Largest size of infarct ≥ 25 mm	5.01	[1.95-12.85]	2.40	3.36	0.001
Thickness-to-volume ratio ≥ 0.043	3.76	[1.16-12.23]	2.26	2.21	0.027
Constant	0.37	[0.19-0.73]	0.12	-2.89	0.004
B. IUGR severity					
Involvement percentage with infarct ≥ 10%	26.73	[2.77-257.76]	30.91	2.84	0.004
Placental globular shape	5.40	[1.13-25.75]	4.30	2.12	0.034
Constant	0.04	[0.01-0.42]	0.05	-2.71	0.007
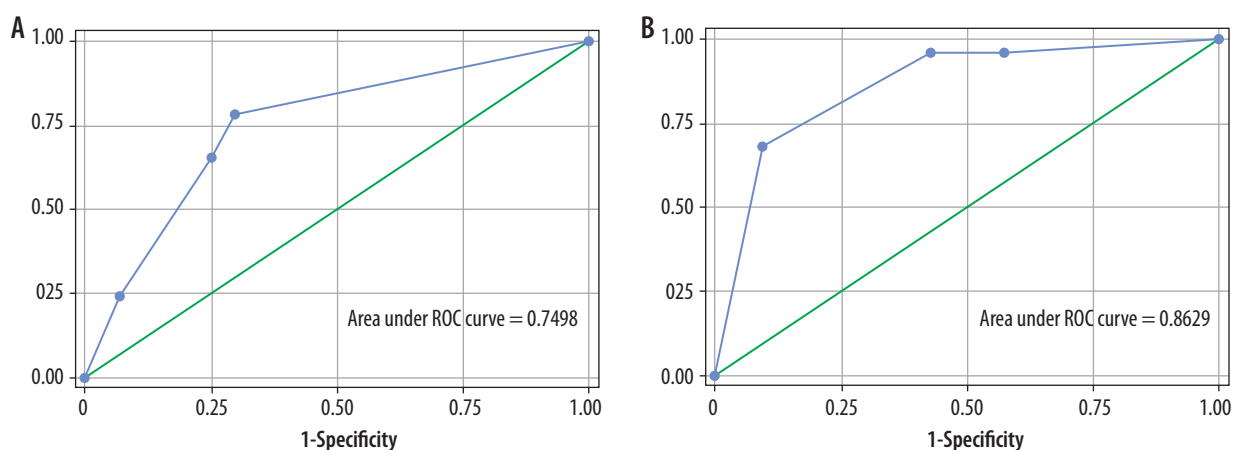
Figure 4. ROC curves for the proposed models regarding (**A**) IUGR diagnosis and (**B**) IUGR severity assessment
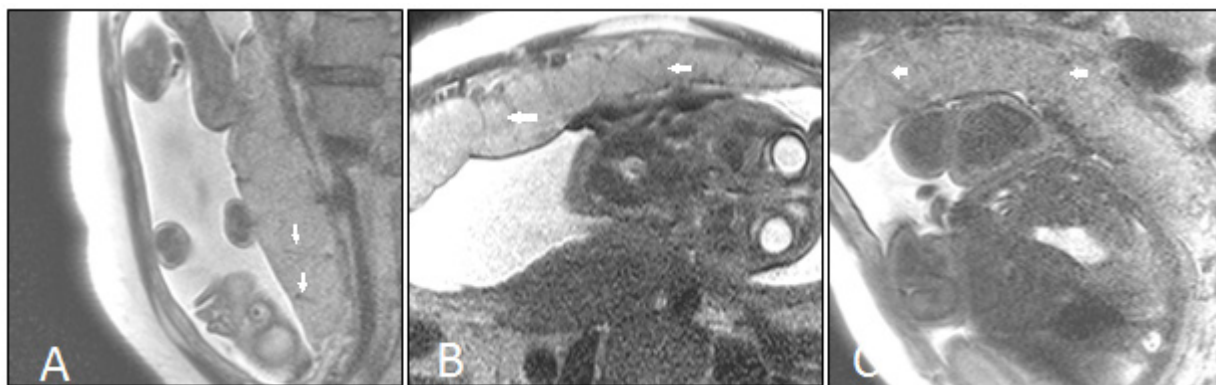
Figure 5. A-C) Single-shot fast spin-echo (SSFSE) MRI sequence of 3 non-IUGR fetuses at 27, 30, and 36 weeks of their gestational age, respectively. These images depict normal evolution of placenta; its general heterogeneity has slightly increased in the third trimester compared to the second trimester. Also, the hypointense-lines perpendicular to placenta plane, represent the interlobular septa (arrows) and denote cotyledon

the capillaries, preferably identified on single-shot spin-echo (SSFSE) MRI sequences (Figure 5). On the other hand, a placental infarct consists of necrosis of a foetal cotyledon caused by occlusion of the supplying uteroplacental artery. However, as previously mentioned in the method section, placental infarcts are areas of low T2 signal or sometimes high T2 intensity with low signal rim, usually in the background of presence of a thick placenta [28].

In a study by Damodaram *et al.*, all pregnancies that ended in perinatal mortality had thickened globular placenta at the time of MRI scan [13]. Also, increased placental maximal thickness-to-volume ratio, which is a reflection of decline in placental surface area, was noted in IUGR cases [13]. Likewise, in our IUGR prediction model, this parameter, alongside the largest infarct size of more than 25 mm, was distinguished as an independent predictor of growth restriction.

Previous studies utilizing placental MRI have identified different parameters of numerous MRI sequences for placental insufficiency in foetuses with IUGR. For instance, a recent study implementing DWI and magnetic resonance spectroscopy proposed a combination of placental ADC values and choline/lipid ratio to be significantly associated with placental

insufficiency to a great diagnostic value (AUC = 0.939) [29]. However, that study was a pilot study with a limited patient population without addressing these predictors in multivariate analysis. Our prediction models were derived from the relatively larger population by evaluating multiple MRI parameters in univariate and multivariate analyses. Moreover, we developed our models based on T1, T2, and DWI sequences, which has wider availability and higher resolution than magnetic resonance spectroscopy.

We acknowledge the limitations of our study. First, no histopathological examinations were performed to correlate with MRI results. However, ultrasound methods with Doppler measurements, which are the basis of IUGR diagnosis and management, are conducted in our study for the assessment of MRI precision. Second, our limited study population was recruited from solely a single centre. However, it is worth mentioning that our sample size was larger than many of the previously published studies. Third, we did not follow each patient by MRI scans during pregnancy; therefore, we could not detect changes in placental parameters. Fourth, we did not provide a validation dataset for our proposed models.

Another limitation was a relatively wide range for the gestational age of included foetuses (weeks 26-39). On the other hand, this wide range can simultaneously ensure good reliability. Although the appropriate time for IUGR screening is during the late weeks of the second trimester, all pregnant women with suspected foetuses should in practice undertake serial follow-up diagnostics. In future, further large-scale multicentric studies are warranted to validate the utility of these models in diverse patient populations.

Conclusions

Placental MRI parameters can differentiate IUGR from AGA and, more precisely, assess the placental insufficiency severity in growth-restricted foetuses. Future studies are required for the validation of the proposed models for IUGR diagnosis and severity assessment.

Disclosure

The authors report no conflict of interest.

References

1. von Beckerath AK, Kollmann M, Rotky-Fast C, et al. Perinatal complications and long-term neurodevelopmental outcome of infants with intrauterine growth restriction. Am J Obstet Gynecol 2013; 208: 130.e1-6. doi: https://doi.org/10.1016/j.ajog.2012.11.014.

2. Lausman A, Kingdom J. Intrauterine growth restriction: screening, diagnosis, and management. J Obstet Gynaecol Can 2013; 35: 741-748.

3. Pijnenborg R, Vercruysse L, Hanssens M. The uterine spiral arteries in human pregnancy: facts and controversies. Placenta 2006; 27: 939-958.

4. Bhide A, Acharya G, Bilardo CM, et al. ISUOG practice guidelines: use of Doppler ultrasonography in obstetrics. Ultrasound Obstet Gynecol 2013; 41: 233-239.

5. Boers KE, Vijgen SM, Bijlenga D, et al. Induction versus expectant monitoring for intrauterine growth restriction at term: randomised equivalence trial (DIGITAT). BMJ 2010; 341: c7087. doi: https://doi.org/10.1136/bmj.c7087.

6. Backe B, Nakling J. Effectiveness of antenatal care: a population based study. Br J Obstet Gynaecol 1993; 100: 727-732.

7. Devoe LD, Gardner P, Dear C, Faircloth D. The significance of increasing umbilical artery systolic-diastolic ratios in third-trimester pregnancy. Obstet Gynecol 1992; 80: 684-687.

8. Powell MC, Buckley J, Price H, et al. Magnetic resonance imaging and placenta previa. Am J Obstet Gynecol 1986; 154: 565-569.

9. Teo TH, Law YM, Tay KH, et al. Use of magnetic resonance imaging in evaluation of placental invasion. Clin Radiol 2009; 64: 511-516.

10. Taillieu F, Salomon LJ, Siauve N, et al. Placental perfusion and permeability: simultaneous assessment with dual-echo contrast-enhanced MR imaging in mice. Radiology 2006; 241: 737-745.

11. Linduska N, Dekan S, Messerschmidt A, et al. Placental pathologies in fetal MRI with pathohistological correlation. Placenta 2009; 30: 555-559.

12. Bonel HM, Stolz B, Diedrichsen L, et al. Diffusion-weighted MR imaging of the placenta in fetuses with placental insufficiency. Radiology 2010; 257: 810-819.

13. Damodaram M, Story L, Eixarch E, et al. Placental MRI in intrauterine fetal growth restriction. Placenta 2010; 31: 491-498.

14. Görkem SB, Coşkun A, Eşlik M, et al. Diffusion-weighted imaging of placenta in intrauterine growth restriction with worsening Doppler US findings. Diagn Interv Radiol 2019; 25: 280-284.

15. Goodyear MD, Krleza-Jeric K, Lemmens T. The Declaration of Helsinki. BMJ 2007; 335: 624-625.

16. Kiserud T, Benachi A, Hecher K, et al. The World Health Organization fetal growth charts: concept, findings, interpretation, and application. Am J Obstet Gynecol 2018; 218 (2 Suppl): S619-s629. doi: https://doi.org/10.1016/j.ajog.2017.12.010.

17. Ciobanu A, Wright A, Syngelaki A, et al. Fetal Medicine Foundation reference ranges for umbilical artery and middle cerebral artery pulsatility index and cerebroplacental ratio. Ultrasound Obstet Gynecol 2019; 53: 465-472.

18. Moradi B, Nezhad ZA, Saadat NS, et al. Apparent diffusion coefficient of different areas of brain in foetuses with intrauterine growth restriction. Pol J Radiol 2020; 85: e301-e308. doi: https://doi.org/10.5114/pjr.2020.96950.

19. Chartier AL, Bouvier MJ, McPherson DR, et al. The Safety of Maternal and Fetal MRI at 3 T. AJR Am J Roentgenol 2019; 213: 1170-1173.

20. Kanal E, Barkovich AJ, Bell C, et al. ACR guidance document on MR safe practices: 2013. J Magn Reson Imaging 2013; 37: 501-530.

21. Derwig I, Lythgoe DJ, Barker GJ, et al. Association of placental perfusion, as assessed by magnetic resonance imaging and uterine artery Doppler ultrasound, and its relationship to pregnancy outcome. Placenta 2013; 34: 885-891.

22. Brunelli R, Masselli G, Parasassi T, et al. Intervillous circulation in intra-uterine growth restriction. Correlation to fetal well being. Placenta 2010; 31: 1051-1056.

23. Sohlberg S, Mulic-Lutvica A, Olovsson M, et al. Magnetic resonance imaging-estimated placental perfusion in fetal growth assessment. Ultrasound Obstet Gynecol 2015; 46: 700-705.

24. Biswas S, Ghosh SK. Gross morphological changes of placentas associated with intrauterine growth restriction of fetuses: a case control study. Early Hum Dev 2008; 84: 357-362.

25. Kaufmann P, Black S, Huppertz B. Endovascular trophoblast invasion: implications for the pathogenesis of intrauterine growth retardation and preeclampsia. Biol Reprod 2003; 69: 1-7.

26. Ishihara N, Matsuo H, Murakoshi H, et al. Increased apoptosis in the syncytiotrophoblast in human term placentas complicated by either preeclampsia or intrauterine growth retardation. Am J Obstet Gynecol 2002; 186: 158-166.

27. Levy R, Smith SD, Yusuf K, et al. Trophoblast apoptosis from pregnancies complicated by fetal growth restriction is associated with enhanced p53 expression. Am J Obstet Gynecol 2002; 186: 1056-1061.

28. Vişan V, Balan RA, Costea CF, et al. Morphological and histopathological changes in placentas of pregnancies with intrauterine growth restriction. Rom J Morphol Embryol 2020; 61: 477-483.

29. Song F, Wu W, Qian Z, etal. Assessment of the Placenta in Intrauterine Growth Restriction by Diffusion-Weighted Imaging and Proton Magnetic Resonance Spectroscopy. Reprod Sci 2017; 24: 575-581.